Catalytic conversion of CO_2 into propylene carbonate in a continuous fixed bed reactor by immobilized ionic liquids

Liying Guo, [iD] * Lili Deng, Xianchao Jin, Yirong Wang and Haozhi Wang

In this study, functionalized composite catalysts, namely, ILs (ILX/(ZnBr$_2$)$_2$), with hydroxyl, carboxyl and amino groups immobilized on a molecular sieve (MCM-22) support were synthesized with the help of a silane coupling agent, 3-chloropropyltriethoxysilane (CPTES). Cycloaddition of CO_2 and propylene oxide (PO) was carried out in a fixed bed reactor. The results show that MCM-22-CPTES-[AeMIM][Zn$_2$Br$_5$] demonstrates the best catalytic properties for this reaction. A high selectivity and yield of propylene carbonate (PC) could be reached at 130 °C under a CO_2 pressure of 2.0 MPa, with a LHSV of 0.75 h^{-1} and a molar ratio of CO_2/PO of 3 : 1. The yield stabilized at 61.6% after 50 h in the fixed bed reactor.
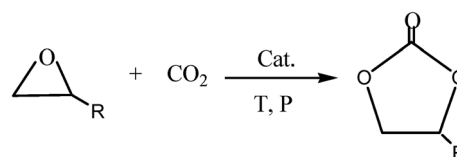
1 Introduction

Carbon dioxide (CO_2) is an attractive C1 source and has gained increasing worldwide attention as a raw material for sequestration and subsequent utilization.[1–3] In view of reducing our carbon footprint, there has been increased research directed towards new methods of CO_2 utilization.[4,5] Numerous techniques have been developed for the preparation of these molecules, one of the most attractive synthetic pathways involves the cycloaddition of CO_2 and epoxides to form cyclic carbonates.[6–10] Scheme 1 shows the reaction used to synthesize cyclic carbonates. Propylene carbonate (PC) is a prominent example among these cyclic carbonates. PC can be employed as a plasticizer for novel mesoporous soft solid electrolytes,[11] as an electrolytic component of electrolyte in lithium batteries[12,13] and as an intermediate to produce polycarbonate[14] on account of its high biodegradability and solvency, high flash and boiling points, low odor and evaporation rate.[15–17] It also has applications in organic synthesis, such as the production of dimethyl carbonate (DMC) through transesterification with methanol.[18]

Conventionally, homogeneous catalysts have been investigated for the synthesis of cyclic carbonates; the most common catalysts for this purpose are alkali metal,[19,20] transition metal complexes[21,22] and ILs.[23–26] Generally, homogeneous catalysts are superior to heterogeneous catalysts in catalytic performances. However, homogeneous catalysts suffer from some drawbacks such as the large amount of catalyst required for the reaction, low stability, harsh reaction conditions and separation of catalyst from the products.[27–29] Hence, the use of heterogeneous catalysts is the preferred choice for cycloaddition reactions. The development of an effective heterogeneous catalytic

system that can overcome these problems and catalyze the cycloaddition of CO_2 and epoxides remains an open challenge. Recently, immobilized IL catalysts have become the focus of many studies as they are easily separable after the reaction and can be reused in subsequent cycles.[30,31] ILs have generally been immobilized on silica gel,[32,33] polymers[8,34,35] and molecular sieves[36,37] because of their large specific surface area, high pore volume, and easy availability.

Although immobilized IL catalysts show excellent catalytic performance in cycloaddition reactions, they are primarily applied in a batch reactor and must be disassembled after each reaction.[32–37] Hence, it is crucial to devise heterogeneously immobilized IL catalysts that can be used for continuous catalysis in fixed bed reactor because there are many attractive features in fixed bed reactors, particularly the realization of large scale production under continuous operating conditions. To the best of our knowledge, Takahashi et al.[33] first reported the continuous operation of immobilized IL catalysts in a fixed bed reactor. The conversion of the epoxide was 80%, but the reaction pressure was as high as about 10 MPa. Xiong et al.[38] prepared ILs immobilized on coconut shell activated carbon (CSAC) as catalysts. These catalysts were used in the cycloaddition of CO_2 to epichlorohydrin (ECH) in a fixed bed reactor and showed excellent catalytic performances; the conversion of ECH was high for these immobilized IL catalysts after 50 h. Fang et al.[39] prepared an efficient catalyst comprising PS-

School of Petrochemical Engineering, Shenyang University of Technology, Liaoyang 111003, P. R. China. E-mail: lyguo1981@163.com

Scheme 1 Synthesis of cyclic carbonates from epoxides and CO_2.

MimCl, $ZnBr_2$ and phenol formaldehyde resin, and applied it for PC synthesis from CO_2 and PO in a fixed bed reactor. The as-prepared catalyst was applied for a 72 h reaction and demonstrated good selectivity and yield of PC.

In this study, we report three composite ILs, namely, [HeMIM]Cl/$(ZnBr_2)_2$, [CeMIM]Cl/$(ZnBr_2)_2$ and [AeMIM] [Zn_2Br_5],[37] covalently immobilized on a molecular sieve (MCM-22) support with the help of a silane coupling agent, 3-chloropropyltriethoxysilane (CPTES). These composites exhibited good chemical and thermal stability, and were applied as novel heterogeneous catalysts in the preparation of PC through the cycloaddition of CO_2 and PO. In addition, flexible automation, process reliability and low mechanical consumption were easily achieved in continuous industrial operation.

2 Experimental

2.1 Reagents

N-Methyl imidazole (99.0%), chloroethanol (99.0%), chloro-acetic acid (99.0%), 2-bromoethylamine hydrogen bromide salt, zinc bromide (98.0%), toluene (99.5%), acetonitrile (99.0%), and propylene oxide (99.5%), used in this study, were of analytic grade and purchased from Sinopharm Chemical Reagent Co., Ltd. (China). 3-Chloropropyltriethoxysilane (CPTES, 95%) was purchased from Aladdin Chemical Co. CO_2 gas (99.95%) was offered by Petrochina Liaoyang Yifang Petrochemical Company (China). MCM-22 was provided by Petrochina Fushun Petrochemical Company (China). All materials were used without further purification.

2.2 Characterization of MCM-22-CPTES-ILX/$(ZnBr_2)_2$

Fourier transform infrared (FT-IR) spectra of MCM-22-CPTES-ILX/$(ZnBr_2)_2$ catalysts were recorded on a MAGNA-IR750 from Thermo Nicolet Corporation. The powder X-ray diffraction (XRD) patterns were obtained using Rigaku Miniflex patterns from Rigaku Corporation. A scan speed of $5°$ min^{-1} was used for the X-ray diffractometer over a scan range of 10–80°. Thermogravimetric analysis (TGA) was conducted using a PerkinElmer TGA4000 instrument. The morphology and surface structure of the molecular sieve was obtained with a Quanta 450 Sigma field emission scanning electron microscope (FE-SEM). The loading mass of ILs and Zn were investigated by elemental analysis and ICP. Then, the purity of PC was

determined by 1790F gas chromatography from Agilent Technologies. The catalytic experimental fixed bed reactor (Tianjin Pengxiang Technology Co., Ltd, China) was used for the catalytic process.

2.3 Preparation of MCM-22-CPTES-ILX/$(ZnBr_2)_2$

2.3.1 Synthesis of MCM-22-CPTES. CPTES (3.5 mL) was slowly added into a flask containing a mixture of MCM-22 (3.5 g) and toluene (50 mL) solvent to prepare MCM-22-CPTES. The reaction mixture was refluxed at 110 °C for 24 h, following which the flask was cooled at room temperature. The solvent was removed by distillation and the solid product was washed three times with ethyl acetate and then dried at 80 °C for 12 h under vacuum to obtain MCM-22-CPTES (4.2 g).

2.3.2 Synthesis of ILX/$(ZnBr_2)_2$. The preparation of [HeMIM]Cl/$(ZnBr_2)_2$, [CeMIM]Cl/$(ZnBr_2)_2$ and [AeMIM][Zn_2Br_5] was conducted according to previously published methods.[37,40,41]

2.3.3 Synthesis of MCM-22-CPTES-ILX/$(ZnBr_2)_2$. ILX/$(ZnBr_2)_2$ (14.5 mmol) and MCM-22-CPTES (4.2 g) were poured into a flask with acetonitrile solvent. The intermixture was refluxed at 80 °C for another 24 h, following which the solvent was removed from the reaction by distillation, finally giving MCM-22-CPTES-ILX/$(ZnBr_2)_2$ catalysts.[34,42] The synthesis procedure of MCM-22-CPTES-ILX/$(ZnBr_2)_2$ is illustrated in Scheme 2.

2.4 Typical procedure for the synthesis of PC from PO and CO_2

The cycloaddition reaction of CO_2 and PO was carried out in a fixed bed reactor. The catalyst was placed in the middle of the packed column and both ends were filled with quartz granules. Then, the fixed bed reactor was sealed and placed under nitrogen (N_2) atmosphere. CO_2 was fed into the fixed bed reactor from a high pressure cylinder, while propylene oxide was fed through a pump. PO was heated in the preheater and into the packed column to react with CO_2; no additional solvent was added during the reaction. The reaction temperature and the pressure were investigated for optimization. The products were analyzed on a gas chromatograph, equipped with a FID and SE-54 column, to calculate selectivity and yield.
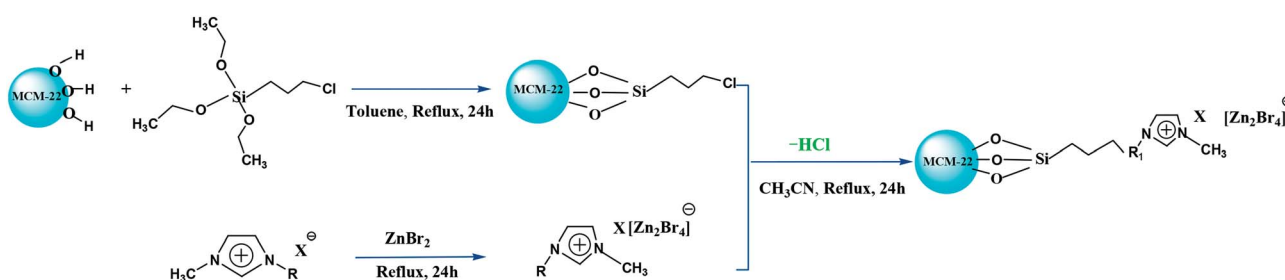
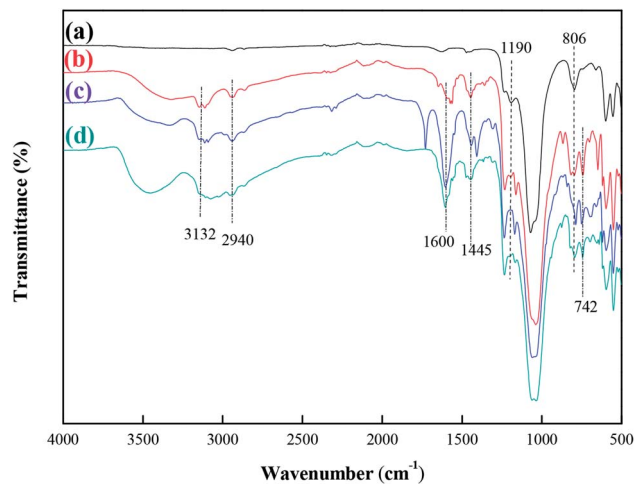**Scheme 2** Synthesis of MCM-22-CPTES-ILX/$(ZnBr_2)_2$ catalysts.

Fig. 1   FT-IR spectra of (a) MCM-22. (b) MCM-22-CPTES-[HeMIM]Cl/$(ZnBr_2)_2$. (c) MCM-22-CPTES-[CeMIM]Cl/$(ZnBr_2)_2$ and (d) MCM-22-CPTES-[AeMIM][Zn_2Br_5].
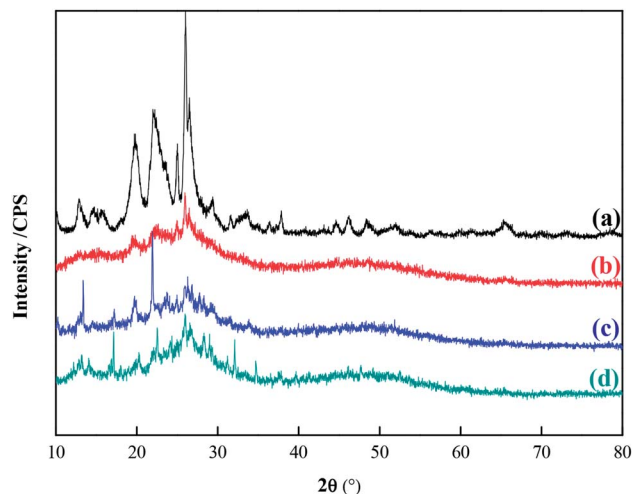

Fig. 2   XRD of (a) MCM-22. (b) MCM-22-CPTES-[HeMIM]Cl/$(ZnBr_2)_2$. (c) MCM-22-CPTES-[CeMIM]Cl/$(ZnBr_2)_2$ and (d) MCM-22-CPTES-[AeMIM][Zn_2Br_5].

3   Results and discussion

3.1   Characterization of MCM-22-CPTES-ILX/$(ZnBr_2)_2$

3.1.1   FT-IR. Fig. 1 shows the FT-IR spectra of different catalysts; it can be seen that the bands at 1190 cm^{-1} and 806 cm^{-1} are typical Si–O peaks from the MCM-22.[43,44] For immobilized ILX/$(ZnBr_2)_2$ catalysts, we observe peaks at 3132 cm^{-1} and 2940 cm^{-1}, which are characteristic peaks assigned to stretching vibrations of CH_3 and CH_2. We also observe three characteristic peaks at 1600 cm^{-1}, 1445 cm^{-1} and 742 cm^{-1} that can be associated with the stretching frequency of the imidazole ring. The hydroxyl peak broadening in the range of 3300–3500 cm^{-1} is associated with water molecules adsorbed on the catalyst surface.[45] The functional groups of ILX/$(ZnBr_2)_2$ were occupied during the preparation of immobilized ILs catalysts, so the hydroxyl, amino and carboxyl peaks were not present. All the observed vibrational peaks indicate the successful immobilization of ILX/$(ZnBr_2)_2$.

3.1.2   XRD. The XRD patterns of MCM-22 and its immobilized ILX/$(ZnBr_2)_2$ catalysts are shown in Fig. 2. The absence of obvious characteristic peaks of the immobilized catalysts in comparison with the support in the XRD patterns suggests that the acidic HCl gas released may dilapidate its initial crystalline structure when ILX/$(ZnBr_2)_2$ bonded with the molecular sieve through the silane coupling agent.[46] The peak intensity of the immobilized IL catalyst was weaker compared with MCM-22 at the corresponding position owing to the intensity of the diffraction peak, which was related to the filling of the hole and the scattering contrast between the hole center and the pore wall.[47,48] As the IL entered the support channel or surface, the scattering contrast weakened resulting in a decrease in the diffraction intensity. In addition, there were irregular crystalline peaks from 39° to 56° for immobilized ILX/$(ZnBr_2)_2$ catalysts, which is due to the addition of the silane coupling agent, CPTES. It appears that ILX/$(ZnBr_2)_2$ is well dispersed on the surface in the channels of the molecular sieve, and the main

bond between the ILX/$(ZnBr_2)_2$ and MCM-22-CPTES was through chemical covalent bonding.

3.1.3   Thermogravimetric analysis (TGA). In order to avoid degradation of the catalysts and to avoid contamination of the catalytic products, it is very important to develop the thermal stability of the immobilized ILX/$(ZnBr_2)_2$ catalysts. Thus, these immobilized catalysts were further characterized by TGA and found to be thermally stable up to 600 °C (Fig. 3). For MCM-22, the weight loss in the investigated temperature range was almost negligible. In addition, these catalysts decomposed in two steps.[8,49,50] The first step in the decomposition was attributed to the successive cleavage of grafted ILX/$(ZnBr_2)_2$ and the second major decomposition step was attributed to the decomposition of a small amount of MCM-22 supporter. The above results evidenced that ILX/$(ZnBr_2)_2$ could endure temperatures of about 300 °C, which manifested that the as-
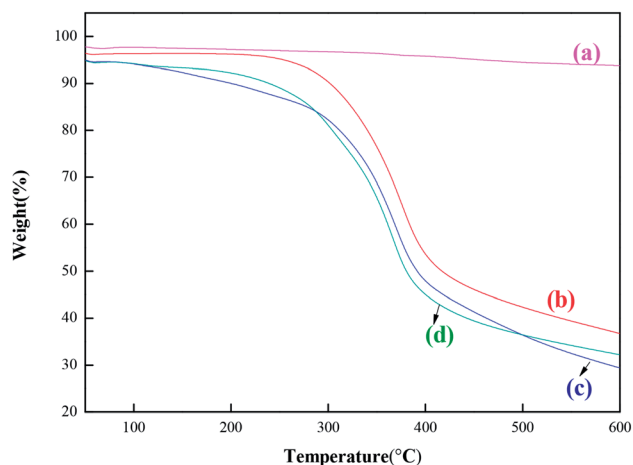

Fig. 3   TG of (a) MCM-22. (b) MCM-22-CPTES-[HeMIM]Cl/$(ZnBr_2)_2$. (c) MCM-22-CPTES-[CeMIM]Cl/$(ZnBr_2)_2$ and (d) MCM-22-CPTES-[AeMIM][Zn_2Br_5].

synthesized catalysts have sufficient thermal stability. The sample MCM-22 began to decompose when temperatures exceeded 460 °C, which indicates that the support material possessed high thermal stability.

3.1.4 SEM and EA. Fig. 4 illustrates the FE-SEM images of the obtained samples of MCM-22-(a), MCM-22-CPTES-[HeMIM]Cl/(ZnBr$_2$)$_2$-(b), MCM-22-CPTES-[CeMIM]Cl/(ZnBr$_2$)$_2$-(c) and MCM-22-CPTES-[AeMIM][Zn$_2$Br$_5$]-(d). As observed in the figures, there are many pores on the surface of MCM-22. Apparently, the immobilized ILX/(ZnBr$_2$)$_2$ catalysts demonstrated some agglomeration, which was different from the observation of the sample of MCM-22 at the same magnification.[7,8,51] This can be regarded as an effective evidence for the successful support of ILX/(ZnBr$_2$)$_2$ on MCM-22. It can be clearly observed that the surface of the immobilized ILX/(ZnBr$_2$)$_2$ is smooth. Probably, ILX/(ZnBr$_2$)$_2$ was introduced randomly on the surface and into the channel. This is consistent with the XRD results which showed a weakened intensity of the diffraction peak. However, the abovementioned phenomenon indicates that the ILX/(ZnBr$_2$)$_2$ immobilization process ultimately results in the presence of the catalyst with a solid form. To determine the elemental composition of the as-prepared MCM-22-CPTES-ILX/(ZnBr$_2$)$_2$, elemental analysis and ICP were carried out and the results are listed in Table 1. It was found that the range of IL present was 1.0–1.5 mmol g^{-1}. In addition, the amount of nitrogen and zinc in the as-synthesized catalyst drastically increased compared to that in the sample of MCM-22, indicating that imidazole was effectively immobilized through covalent bonding.

3.2 Catalytic activity of immobilized ILX/(ZnBr$_2$)$_2$

3.2.1 Effect of reaction temperature. The cycloaddition reaction of CO$_2$ and PO was carried out in a fixed bed reactor without the use of solvent, which would be affected by temperature, as shown in Fig. 5. A temperature range of 100–140 °C was investigated under the pressure of 2.0 MPa. It was noticed that the as-synthesized catalysts not only showed high PC selectivity, but also displayed more significant PC yield with an increase in temperature. The yield of PCs are 62.2%, 65.4% and 70.3% for MCM-22-CPTES-[HeMIM]Cl/(ZnBr$_2$)$_2$, MCM-22-CPTES-[CeMIM]Cl/(ZnBr$_2$)$_2$ and MCM-22-CPTES-[AeMIM][Zn$_2$Br$_5$], respectively. When the temperature was increased, both CO$_2$ and PO could easily reach the catalyst surface, leading to a rapid increase in the yield.[24] However, the selectivity and yield declined at 140 °C because the reaction produced byproducts, such as polymers, at higher temperature.[51] On the basis of these results, we see that the MCM-22 immobilized ILX/(ZnBr$_2$)$_2$ catalysts exhibited stabilized catalytic performance in a continuous fixed bed reactor, which is comparable to those reported in the batch reactor.[32–37,51]
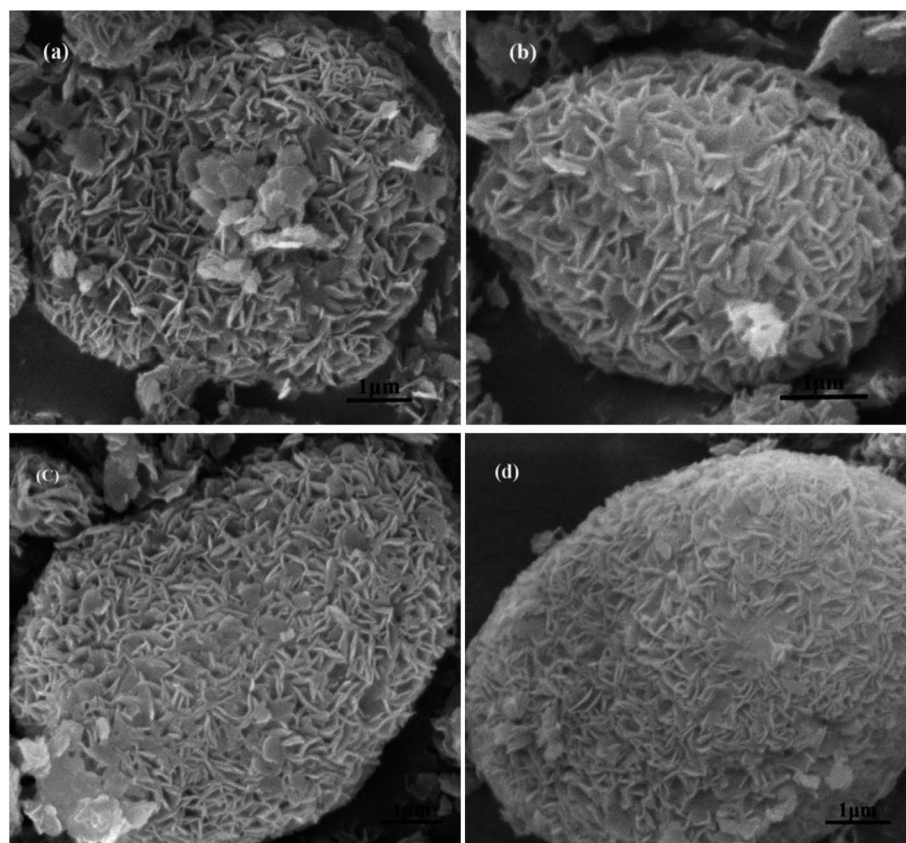

Fig. 4 SEM of MCM-22 and MCM-22-CPTES-ILX/(ZnBr$_2$)$_2$. (The morphology characterizations of (a) MCM-22 and (b–d) MCM-22-CPTES-ILX/(ZnBr$_2$)$_2$).

Table 1 Amount of immobilized IL calculated from elemental analysis

Catalyst	N (wt%)	C (wt%)	H (wt%)	IL grafted [mmol g^{-1}]	Zn^c [mmol g^{-1}]
MCM-22	—	—	—	—	—
MCM-22-CPTES-[HeMIM]Cl/(ZnBr$_2$)$_2$	3.98	13.64	3.55	1.42	2.79
MCM-22-CPTES-[CeMIM]Cl/(ZnBr$_2$)$_2$	3.75	13.01	3.29	1.34	2.61
MCM-22-CPTES-[AeMIM][Zn$_2$Br$_5$]^a	4.87	12.26	3.27	1.16	2.29
MCM-22-CPTES-[AeMIM][Zn$_2$Br$_5$]^b	3.91	11.73	2.26	0.93	1.64

^{a} Fresh catalyst. ^{b} Reaction after 50 h. ^{c} Zn loading obtained from ICP analysis.

3.2.2 Effect of reaction pressure. Fig. 6 shows significant effects of pressure in the range of 1.0–3.0 MPa on the cycloaddition reaction at 130 °C. In this reaction, the pressure was modulated by altering the pressure of CO_2, while PO was conveyed with a constant flow rate in the experiments. It was found that an increase in CO_2 pressure resulted in a moderate increase in PC yield when the pressure was low, but a decrease in the yield was observed as the pressure increased. The effect of the change in CO_2 pressure on catalytic activity has been previously studied in other catalytic systems.[32–37,51] For this cycloaddition reaction the optimal conditions would be 130 °C and 2.0 MPa over the MCM-22 immobilized ILX/(ZnBr$_2$)$_2$ catalysts in the fixed bed reactor and the optimal catalyst was MCM-22-CPTES-[AeMIM]Br/(ZnBr$_2$)$_2$. Based on the reported mechanism,[8,36,51] the immobilized ILX/(ZnBr$_2$)$_2$ initially interacts with epoxides and the anion of ILX/(ZnBr$_2$)$_2$, as an anionic nucleophile, could attack the β-carbon atom of PO due to its low steric hindrance. The H atom of the functionalized group of ILX/(ZnBr$_2$)$_2$ interacts with the O atom of PO by means of hydrogen bonding and then, the intermediate combines with CO_2. In comparison, hydroxyl, carboxyl or amino groups of functionalized ILX/(ZnBr$_2$)$_2$ would remove a hydrogen atom during the immobilization process. Only the amino group retained a hydrogen atom after [AeMIM]Br/(ZnBr$_2$)$_2$ was immobilized on MCM-22 with the help of the silane coupling agent (CPTES). According to the references,[36,42] it is reported that anion movement away from the imidazolium cation of IL could be in the order of I$^-$ > Br$^-$ > Cl$^-$, which is also in accordance with their nucleophilicity and provides a significant theoretical basis to imply that MCM-22-CPTES-[AeMIM][Zn$_2$Br$_5$] would exhibit the highest catalytic performance among the investigated catalysts.

3.2.3 Effect of liquid hourly space velocity (LHSV). The change in catalytic activity with the liquid hourly space velocity (LHSV) is shown in Fig. 7. At lower LHSV, the yield of PC remains basically unchanged. When LHSV increased, the residence time of the feedstock decreased in the fixed bed reactor, which might cause self-polycondensation for PO. In the case of high temperatures, the selectivity declined and the yield of PC decreased with the increase in LHSV.[30] LHSV stabilized at 0.75 h^{-1}, which was chosen as the optimal value for this catalytic system.

3.2.4 Effect of the molar ratio of CO_2/PO. To elucidate the impact of the molar ratio of CO_2/PO, the reaction was conducted over a range from 1.0 to 5.0 mol mol^{-1}. The temperature, pressure and other conditions in this reaction were kept constant. Fig. 8 shows the effect of CO_2/PO on the selectivity and yield. When the molar ratio of CO_2/PO was 1.0 mol mol^{-1}, the yield of PC was 63.4%. As the CO_2/PO ratio reached 3.0 mol mol^{-1}, the yield of PC increased and the highest yield was
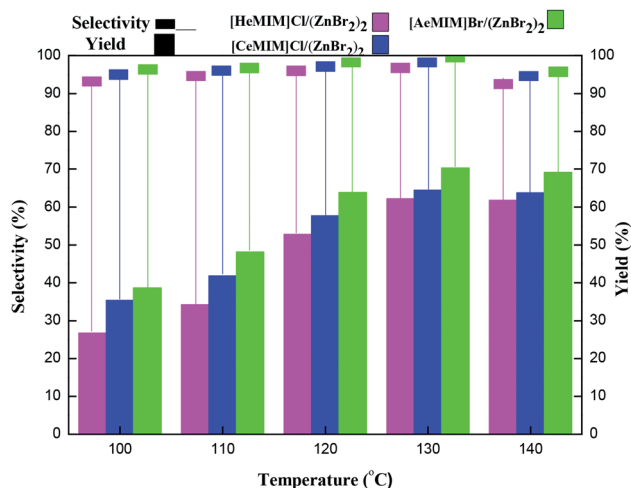

Fig. 5 Effects of temperature on the catalytic performance of MCM-22-CPTES-ILX/(ZnBr$_2$)$_2$. Reaction conditions: pressure, 2.0 MPa; LHSV, 0.75 h^{-1}; CO_2/PO (mol mol^{-1}), 3 : 1; reaction time, 5 h.

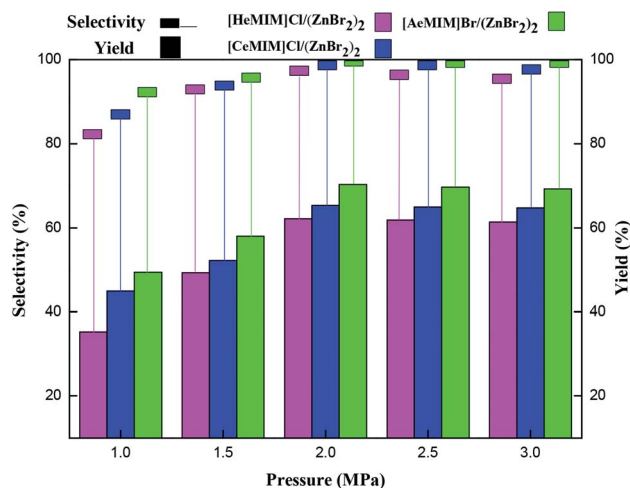**Fig. 6** Effects of pressure on the catalytic performance of MCM-22-CPTES-ILX/(ZnBr$_2$)$_2$. Reaction conditions: temperature, 130 °C; LHSV, 0.75 h^{-1}; CO_2/PO (mol mol^{-1}), 3 : 1; reaction time, 5 h.
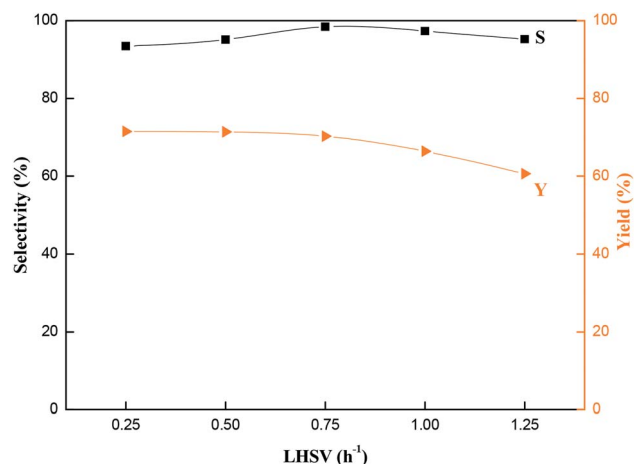
Fig. 7 Effects of LHSV on the catalytic performance of MCM-22-CPTES-[AeMIM][Zn_2Br_5]. Reaction conditions: temperature, 130 °C; pressure, 2.0 MPa; CO_2/PO (mol mol^{-1}), 3 : 1; reaction time, 5 h.
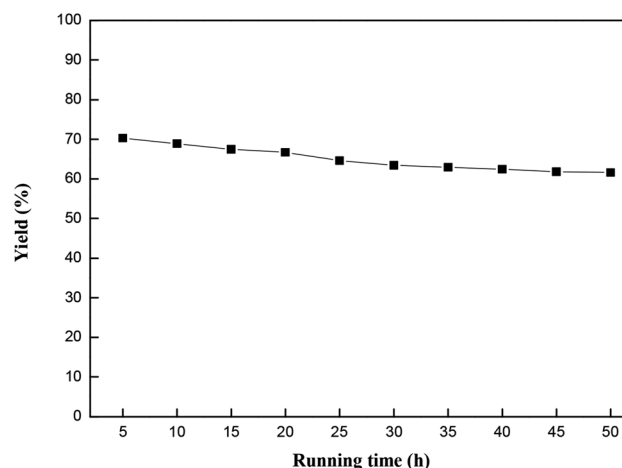

Fig. 9 Effects of reaction time on the catalytic performance of MCM-22-CPTES-[AeMIM][Zn_2Br_5]. Reaction conditions: temperature, 130 °C; pressure, 2.0 MPa; LHSV, 0.75 h^{-1}; CO_2/PO (mol mol^{-1}), 3 : 1.

achieved. At CO_2/PO ratios above this value, we observe that the PC yield decreased. This may be due to the amount of CO_2 becoming larger when the CO_2/PO ratio rises, which significantly affected the reaction.[52] In other words, increasing the CO_2/PO ratio increases the velocity of CO_2 while PO velocity of is kept constant. This results in a small amount of PO leaving the fixed bed due to the CO_2 flow and not being able to participate in the reaction, resulting in an evident decline in the yield of PC.[53]

3.2.5 Reaction time. A short duration reaction using the catalyst MCM-22-CPTES-[AeMIM][Zn_2Br_5] at 130 °C and 2.0 MPa is shown in Fig. 9. The cycloaddition reaction was carried out continuously for 50 h. Initially, it can be seen that the yield of PC decreases slightly. When the reaction time reached 30 h, the yield of PC dropped to 63.4%. However, after 30 h, the yield remains relativity stable. This may be due to a small amount of [AeMIM][Zn_2Br_5] immobilized on the carrier MCM-22 through

physical adsorption; this physical bond is weak and results in IL leaching during the reaction. This phenomenon has also been reported for catalytic reaction processes in batch reactors.[37,51] Furthermore, we also performed FT-IR (Fig. 10) and FE-SEM (Fig. 11) analysis of the MCM-22-CPTES-[AeMIM][Zn_2Br_5] catalyst after 50 h and compared its physicochemical properties with the fresh catalyst. The FT-IR spectrum of the used catalyst revealed that there is no observable morphological damage in this catalyst even after 50 h of reaction. The FE-SEM results were almost identical to those obtained with the FT-IR spectra. Furthermore, in order to confirm that the decrease in catalytic activity was related to IL leaching, we determined the amount of [AeMIM][Zn_2Br_5] after 50 h-reaction and in the fresh catalyst by elemental analysis and the results are shown in Table 1. It can be concluded that the amount of [AeMIM][Zn_2Br_5] grafted on MCM-22 was less after 50 h reaction than in the fresh catalyst. Although this was a very short continuous-reaction experiment,
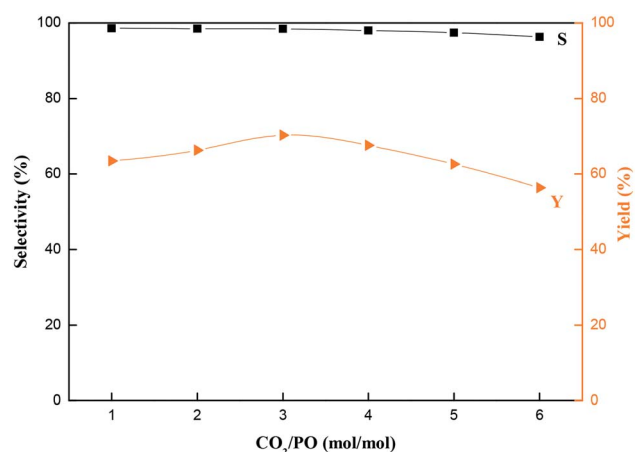

Fig. 8 Effects of the molar ratio of CO_2/PO on the catalytic performance of MCM-22-CPTES-[AeMIM][Zn_2Br_5]. Reaction conditions: temperature, 130 °C; pressure, 2.0 MPa; LHSV, 0.75 h^{-1}; reaction time, 5 h.
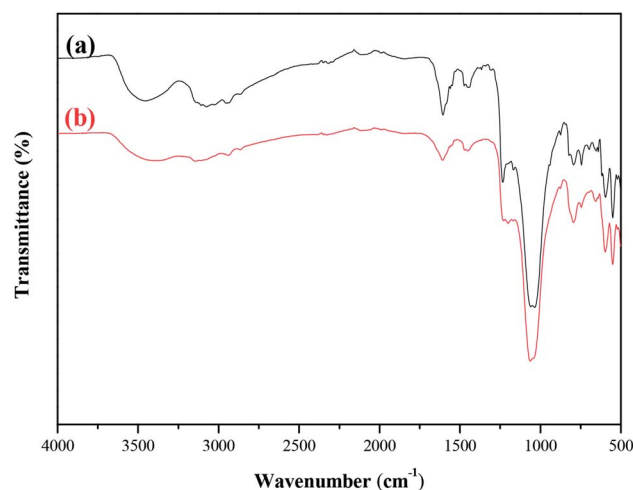

Fig. 10 FT-IR spectra comparison of the fresh and 50 h-reaction-used MCM-22-CPTES-[AeMIM][Zn_2Br_5]. (a) Fresh catalyst (b) after 50 h of reaction.
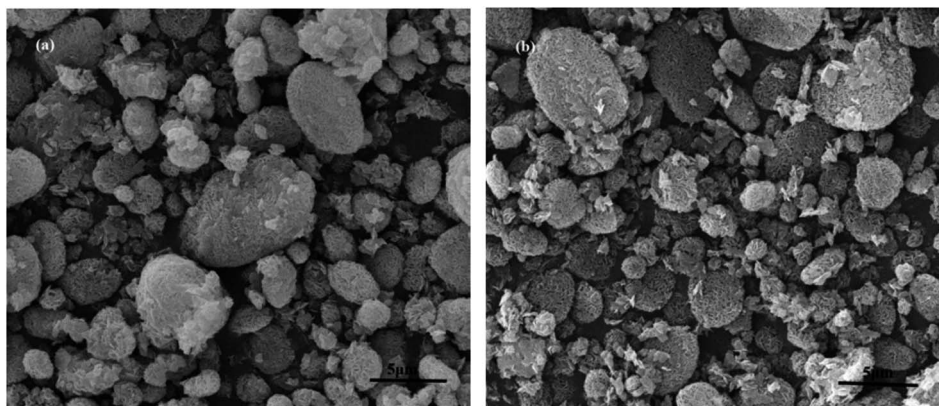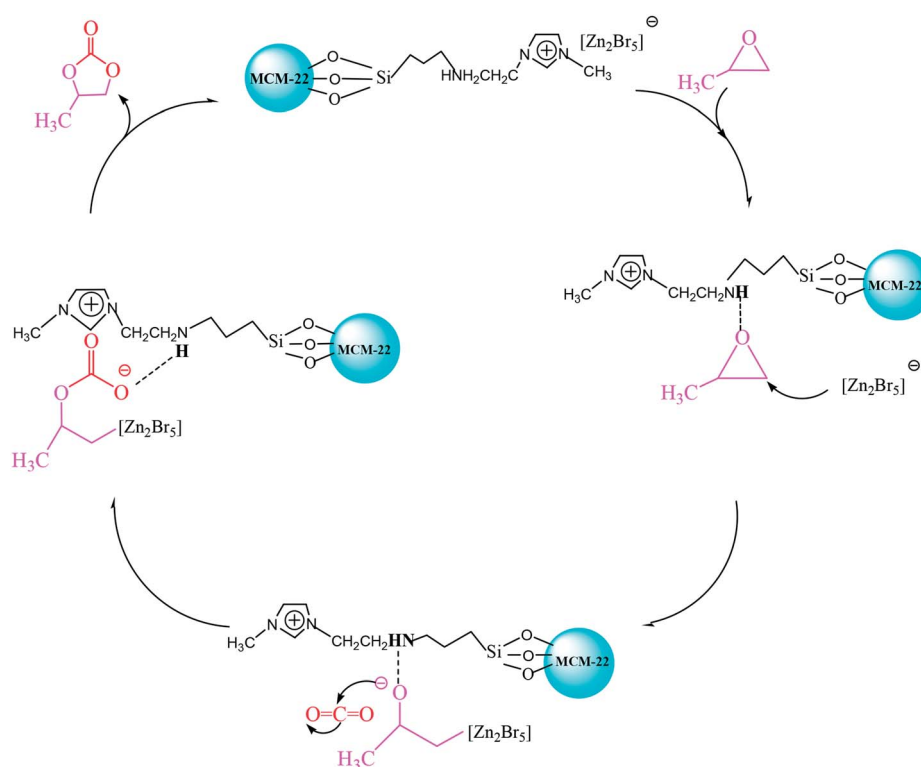
Fig. 11 SEM comparison of the fresh and 50 h-reaction-used MCM-22-CPTES-[AeMIM][Zn_2Br_5]. (a) Fresh catalyst (b) after 50 h of reaction.

Scheme 3 Proposed reaction mechanism for the MCM-22-CPTES-[AeMIM][Zn_2Br_5] catalyzed reaction.

it could demonstrate that the MCM-22 immobilized [AeMIM][Zn_2Br_5] catalyst basically exhibited relatively stable catalytic activity in a fixed bed reactor without considering physical adsorption.

3.2.6 Reaction mechanism. Based on published reports[36,51] and the results in this study, a possible reaction mechanism for fixation of CO_2 with epoxide into cyclic carbonate catalyzed by MCM-22-CPTES-[AeMIM][Zn_2Br_5] is proposed (Scheme 3). First, the oxygen atom of epoxide was activated by hydrogen bond interaction, resulting in the polarization of the C–O bond, which makes the ring opening easier. Simultaneously, the nucleophilic [Zn_2Br_5]$^-$ attack at the less sterically hindered

carbon atom of the epoxide takes place, resulting in an opening of epoxide. Later, the oxygen anion inter-mingled with carbon atom of the CO_2 molecule to form the cyclic carbonate, followed by regeneration of the catalyst.

4 Conclusions

In conclusion, MCM-22 immobilized composite ILs (ILX/($ZnBr_2$)$_2$) with CPTES catalysts were prepared successfully and used in the cycloaddition reaction of CO_2 and PO. Among the three investigated catalysts, MCM-22-CPTES-[AeMIM][Zn_2Br_5] exhibited excellent catalytic performance in the fixed bed reactor. Probably, hydroxyl, carboxyl and amino groups of

functionalized $ILX/(ZnBr_2)_2$ would remove a hydrogen atom in the immobilization process. Hence, only the amino hydrogen can form a hydrogen bond with the O atom of PO, which greatly affects the reaction. The amino, bromide ion and Lewis acid zinc bromide of $ILX/(ZnBr_2)_2$ in the catalyst played essential roles in promoting the catalytic activity and were main reasons for the excellent selectivity and yield of PC using MCM-22-CPTES-[AeMIM][Zn_2Br_5] as a catalyst. We demonstrate a truly heterogeneous and environmentally friendly catalyst that is capable of realizing the continuous catalysis of PC from PO and CO_2 in a solvent-free reaction, which can contribute to a green and environmental protection technology.

Conflicts of interest

There are no conflicts to declare.

Acknowledgements

References

1 W. M. Ren, Z. W. Liu, Y. Q. Wen, R. Zhang and X. B. Lu, *J. Am. Chem. Soc.*, 2009, **131**, 11509–11518.

2 M. Y. He, Y. H. Sun and B. X. Han, *Angew. Chem., Int. Ed.*, 2013, **52**, 9620–9633.

3 Q. Su, X. Q. Yao, W. G. Cheng and S. J. Zhang, *Green Chem.*, 2017, **19**, 2957–2965.

4 W. Z. Zhang, M. W. Yang and X. B. Lu, *Green Chem.*, 2016, **18**, 4181–4184.

5 C. Kohrt and T. Werner, *ChemSusChem*, 2015, **8**, 2031–2034.

6 M. North, R. Pasquale and C. Young, *Green Chem.*, 2010, **12**, 1514–1539.

7 Y. Leng, D. Lu, P. P. Jiang, C. J. Zhang, J. W. Zhao and W. J. Zhang, *Catal. Commun.*, 2016, **74**, 99–103.

8 A. H. Jadhav, G. M. Thorat, K. Lee, A. C. Lim, H. Kang and J. G. Seo, *Catal. Today*, 2016, **265**, 56–67.

9 F. Adam, J. N. Appaturi and E. P. Ng, *J. Mol. Catal. A: Chem.*, 2014, **386**, 42–48.

10 S. M. Sadeghzadeh, *Green Chem.*, 2015, **17**, 3059–3066.

11 C. Chotsuwan, S. Boonrungsiman, T. Chokanarojwong and S. Dongbang, *J. Solid State Electrochem.*, 2017, **21**, 3011–3019.

12 L. F. Zhang, S. Q. Du, Q. L. Song, Y. Liu and S. W. Guo, *Chem. Res. Chin. Univ.*, 2017, **33**, 779–784.

13 J. H. Clements, *Ind. Eng. Chem. Res.*, 2003, **42**, 663–674.

14 P. T. Anastas and R. L. Lankey, *Green Chem.*, 2000, **2**, 289–295.

15 S. Y. Huang, S. G. Liu, J. P. Li, N. Zhao, W. Wei and Y. H. Sun, *Catal. Lett.*, 2006, **112**, 187–191.

16 G. L. Yu, X. R. Chen and C. L. Chen, *React. Kinet. Catal. Lett.*, 2009, **97**, 69–75.

17 T. Sakakura and K. Kohno, *Chem. Commun.*, 2009, **45**, 1312–1330.

18 H. Wang, M. H. Wang, N. Zhao, W. Wei and Y. H. Sun, *Catal. Lett.*, 2005, **105**, 253–257.

19 M. A. Fuchs, C. Altesleben, S. C. Staudt, O. Walter, T. A. Zevaco and E. Dinjus, *Catal. Sci. Technol.*, 2014, **4**, 1658–1673.

20 J. Song, Z. Zhang, B. Han, S. Hu, W. Li and Y. Xie, *Green Chem.*, 2008, **10**, 1337–1341.

21 A. Decortes, A. M. Castilla and A. W. Kleij, *Angew. Chem., Int. Ed.*, 2010, **49**, 9822–9837.

22 T. Ema, Y. Miyazaki, J. Shimonishi, C. Maeda and J. Y. Hasegawa, *J. Am. Chem. Soc.*, 2014, **136**, 15270–15279.

23 J. J. Peng and Y. Q. Deng, *Chin. J. Catal.*, 2001, **22**, 598–600.

24 Y. G. Zhang and J. Y. G. Chan, *Energy Environ. Sci.*, 2010, **3**, 408–417.

25 J. Q. Wang, J. Y. Leong and Y. G. Zhang, *Green Chem.*, 2014, **16**, 4515–4519.

26 F. W. Li, L. F. Xiao, C. G. Xia and B. Hu, *Tetrahedron Lett.*, 2004, **45**, 8307–8310.

27 M. I. Kim, D. K. Kim, K. V. Bineesh, D. W. Kim, M. Selvaraj and D. W. Park, *Catal. Today*, 2013, **200**, 24–29.

28 S. Liang, H. Liu, T. Jiang, J. Song, G. Yang and B. Han, *Chem. Commun.*, 2011, **47**, 2131–2133.

29 D. Bai, S. Duan, L. Hai and H. Jing, *ChemCatChem*, 2012, **4**, 1752–1758.

30 Z. Z. Yang, Y. N. Zhao and L. N. He, *RSC Adv.*, 2011, **1**, 545–567.

31 J. Sun, W. G. Cheng, W. Fan, Y. H. Wang, Z. Y. Meng and S. J. Zhang, *Catal. Today*, 2009, **148**, 361–367.

32 M. I. Kim, S. J. Choi, D. W. Kim and D. W. Park, *J. Ind. Eng. Chem.*, 2014, **20**, 3102–3107.

33 T. Takahashi, T. Watahiki, S. Kitazume, H. Yasuda and T. Sakakura, *Chem. Commun.*, 2006, 1664–1666.

34 J. Sun, J. Q. Wang, W. G. Cheng, J. X. Zhang, X. H. Li, S. J. Zhang and Y. B. She, *Green Chem.*, 2012, **14**, 654–660.

35 J. Sun, W. G. Cheng, W. Fan, Y. H. Wang, Z. Y. Meng and S. J. Zhang, *Catal. Today*, 2009, **148**, 361–367.

36 W. G. Cheng, X. Chen, J. Sun, J. Q. Wang and S. J. Zhang, *Catal. Today*, 2013, **200**, 117–124.

37 L. Y. Guo, L. L. Deng, X. C. Jin, H. Wu and L. Z. Yin, *Catal. Lett.*, 2017, **147**, 2290–2297.

38 Y. L. Zhang, Z. T. Tan, B. L. Liu, D. S. Mao and C. R. Xiong, *Catal. Commun.*, 2015, **68**, 73–76.

39 Z. Z. Zhang, X. L. Sun, X. W. Zhang and X. C. Fang, *Catal. Lett.*, 2016, **146**, 2098–2104.

40 L. Y. Guo, B. Zhang, Z. M. Wang, X. Y. Ma and P. C. Huang, *Acta Polym. Sin.*, 2015, **5**, 556–563.

41 E. H. Lee, J. Y. Ahn, M. M. Dharman, D. W. Park, S. W. Park and I. Kim, *Catal. Today*, 2008, **131**, 130–134.

42 Y. Xie, K. L. Ding, Z. M. Liu, J. J. Li, G. M. An, R. T. Tao, Z. Y. Sun and Z. Z. Yang, *Chem.–Eur. J.*, 2010, **16**, 6687–6692.

43 F. Adam, S. Balakrishnan and P. L. Wong, *J. Phys. Sci.*, 2006, **17**, 1–13.

44 F. Adam, J. N. Appaturi, R. Thankappan and M. A. M. Nawi, *Appl. Surf. Sci.*, 2010, **257**, 811–816.

45 J. N. Appaturi and F. Adam, *Appl. Catal., B*, 2013, **136**, 150–159.

46 M. H. Valkenberg, C. deCastro and W. F. Hölderich, *Green Chem.*, 2002, **4**, 88–93.

47 W. Hammond, E. Prouzet and S. D. Mahanti, *Microporous Mesoporous Mater.*, 1999, **27**, 19–25.

48 M. B. Yue, L. B. Sun and Y. Cao, *Microporous Mesoporous Mater.*, 2008, **114**, 74–81.

49 V. B. Saptal and B. M. Bhanage, *ChemCatChem*, 2016, **8**, 244–250.

50 W. H. Zhang, P. P. He, S. Wu, J. Xu, Y. X. Li, G. Zhang and X. Y. Wei, *Appl. Catal., A*, 2016, **509**, 111–117.

51 W. L. Dai, L. Chen, S. F. Yin, S. L. Luo and C. T. Au, *Catal. Lett.*, 2010, **135**, 295–340.

52 J. Yue, G. W. Chen, Q. Yuan, L. A. Luo and Y. Gonthier, *Chem. Eng. Sci.*, 2007, **62**, 2096–2108.

53 Y. C. Zhao, C. Q. Yao, G. W. Chen and Q. Yuan, *Green Chem.*, 2013, **15**, 446–452.

This journal is © The Royal Society of Chemistry 2018